

Accepted Manuscript

Methane production and fertilizing value of organic waste: organic matter characterization for a better prediction of valorization pathways

Julie Jimenez, Han Lei, Jean-Philippe Steyer, Sabine Houot, Dominique Patureau

PII: S0960-8524(17)30844-1
DOI: <http://dx.doi.org/10.1016/j.biortech.2017.05.176>
Reference: BITE 18202

To appear in: *Bioresource Technology*

Received Date: 13 March 2017
Revised Date: 26 May 2017
Accepted Date: 27 May 2017



Please cite this article as: Jimenez, J., Lei, H., Steyer, J.-P., Houot, S., Patureau, D., Methane production and fertilizing value of organic waste: organic matter characterization for a better prediction of valorization pathways, *Bioresource Technology* (2017), doi: <http://dx.doi.org/10.1016/j.biortech.2017.05.176>

This is a PDF file of an unedited manuscript that has been accepted for publication. As a service to our customers we are providing this early version of the manuscript. The manuscript will undergo copyediting, typesetting, and review of the resulting proof before it is published in its final form. Please note that during the production process errors may be discovered which could affect the content, and all legal disclaimers that apply to the journal pertain.

Comment citer ce document :

Jimenez, J. (Auteur de correspondance), Han, L., Steyer, J.-P., Houot, S., Patureau, D. (2017). Methane production and fertilizing value of organic waste: organic matter characterization for a better prediction of valorization pathways. *Bioresource Technology*, 241, 1012-1021. DOI : 10.1016/j.biortech.2017.05.176

1 **Methane production and fertilizing value of organic waste:**
2 **organic matter characterization for a better prediction of**
3 **valorization pathways**

4 Julie Jimenez¹, Han Lei¹, Jean-Philippe Steyer¹, Sabine Houot², Dominique Patureau¹

5 ¹LBE INRA, UR0050, 102 Avenue des Etangs, Narbonne, F-11100, France

6 ² UMR ECOSYS, INRA, AgroParisTech, Université Paris-Saclay, 78 850 Thiverval-Grignon, France

7 E-mail: julie.jimenez@ inra.fr

8 **Abstract**

9 Organic wastes are potential sources of both energy as well as crop production fertilizers.
10 Correlations and models, involving organic matter characterization, have been previously
11 described by several authors although there is still a lack in knowledge on the potential of
12 simultaneous predictions of methane and organic fertilizer quality to optimize the wastes
13 treatments. A methodology combining chemical accessibility and fluorescence spectroscopy
14 was used to characterise 82 different organic wastes. Characterization data were compared
15 with the biochemical methane potential (BMP), and with the biodegradable organic carbon
16 obtained by soil incubation (C_{bio}). High correlations values were observed (R^2 of 0.818 for
17 BMP and 0.845 for C_{bio}). Model coefficients highlighted the differences and similarities
18 between anaerobic and aerobic soil biodegradation, suggesting that anaerobic recalcitrant
19 molecules could enhance soil fertility. This is a first step in the development of a tool for
20 optimizing both types of valorisation according to agrosystem needs and constraints.

21 **Key words** biodegradability, methane production, soil, fluorescence, accessibility

22 **List of abbreviations**

Abbreviation	Definition	Units
ADM1	Anaerobic Digestion Model N°1	
BMP	Biochemical Methane Potential	$\text{Nm}^3\text{CH}_4\cdot\text{gVS}^{-1}$
C_bio	Biodegradable organic Carbon in soil incubation	%TOC
COD	Chemical Oxygen Demand	$\text{gO}_2\cdot\text{gDS}^{-1}$
DS	Dried Solids	% fresh matter
FFMSW	Fermentescible Fraction of Municipal Solid Wastes	
HCA	Hierarchical Clustering Analysis	
IROC	Indicator of Residual Organic Carbon	% TOC
NIRS	Near InfraRed Spectroscopy	
NEOM	Non Extractible Organic Matter	%COD
OM	Organic Matter	
OR	Organic Residues	
PCA	Principal Component Analysis	
PEOM	Poorly Extractible Organic Matter	%COD
PLS	Partial Least Square regression	
$P_f(i)$	Fluorescence percentage of a zone i	%
R^2	Correlation coefficient from PLS	
REOM	Readily Extractible Organic Matter	%COD
RMSE	Root Mean Square Error	Unit of the predicted variable
RMSEP	Root Mean Square Error of prediction	Unit of the predicted variable
Q^2	Percent of variation of Y predicted by model in cross-validation	
SEOM	Slowly Extractible Organic Matter	%COD
$S(i)$	Area of a zone i from fluorescence spectra	Nm^2
SPOM	Soluble from Particular extractible Organic Matter	%COD
TOC	Total Organic Carbon	$\text{mg C}\cdot\text{gDS}^{-1}$
$V_f(i)$	Normalized fluorescence volume of a zone i	U.A.
$V_{f_raw}(i)$	Raw fluorescence volume of a zone i	U.A.
VS	Volatile Solids	% DS

24 **Introduction**

25 The aim of environmental biorefinery is to establish a complete valorisation of organic
26 wastes, which should turn into valuable organic resources. Indeed, process treatments
27 involved in biorefinery include anaerobic digestion, fermentation, aerobic digestion,
28 composting, thermal conversion, etc... The choice of these treatments depends on the
29 characteristics of the organic residues (OR) and on the targeted services (i.e. energy
30 production, high added value molecules or organic fertilizers).
31 In this study, focus was put on two main services: (i) the production of methane from
32 anaerobic digestion of OR, which could potentially be subsequently used for electricity or
33 heat production and (ii) the use of OR as organic fertilizer on cropped soils whether treated or
34 not, thanks to their content in nutrients and organic carbon.

35 In both cases, the potential interest is related to the biodegradation potential of the organic
36 matter during anaerobic digestion (the higher the biodegradation potential, the greater the
37 methane production) or during aerobic soil incubation (the lower the biodegradation potential,
38 the greater its value as an organic soil amendment).

39 Until present, the quality of digestate for agronomic valorisation has been poor. Management
40 and prediction of anaerobic digestion for methane production would allow for digestate
41 quality control and the availability of this knowledge would improve the optimisation of
42 anaerobic digestion for both targeted services. The main issue to achieve this goal would be
43 to identify relevant actuators for controlling both potentials. These two potentials depend on
44 the chemical characterization of OR as well as its chemical and biodegradability/stability
45 (Angelidaki et al., 2004; Lashermes et al., 2009; Peltre et al., 2014 ;Godin et al., 2015).

46 Indeed, during the past two decades, several authors observed significant correlations between
47 certain indicators based on the chemical composition of OR and the studied potentials
48 (Buffiere et al., 2006; Gunaseelaan et al., 2007 and 2009; Lashermes et al., 2009; Lesteur et

49 al., 2011; Thomsen et al., 2014; Peltre et al., 2014; Thomsen et al., 2014; Godin et al., 2015;
50 Bekiaris et al. 2015 a and b; Kafle et al., 2016; Fitamo et al., 2017). These correlations were
51 used for predicting biological incubation tests which can be resource and time consuming
52 (Godin et al., 2015).

53 Usually, the anaerobic biodegradation potential of an OR is assessed by performing a
54 Biochemical Methane Potential test (BMP) (Angelidaki et al., 2004). During this test, the
55 methane production related to anaerobic biodegradation is measured for at least 30 days
56 (depending on the OR) on a mixture of OR with an anaerobic inoculum under optimal
57 conditions (35°C, addition of metals and nutrients, appropriate substrate : inoculum ratio and
58 bicarbonate buffer). At the end of the incubation period, the cumulated production is assumed
59 to be the methane potential production of the OR. A similar biological incubation test is
60 widely used to assess the aerobic organic carbon degradation of OR during soil incubation
61 under controlled conditions of moisture and temperature, over at least 91 days (Lashermes et
62 al., 2009). A number of authors have applied a chemical characterisation of OR for BMP and
63 soil carbon mineralization prediction. For aerobic biodegradation, an indicator of residual
64 organic carbon (IROC) has been developed by Lashermes et al. (2009) and has been
65 standardized as mentioned by Peltre et al. (2011). It was based on fiber fractionation (Van
66 Soest, 1963) and on the organic carbon fraction mineralized after 3 days of incubation. It has
67 been applied to predict the evolution of soil OM after repeated applications of various organic
68 residues in long-term field experiments (Peltre et al., 2012). Van Soest fractionation has also
69 been successfully used for BMP prediction of lignocellulosic residues (Buffiere et al., 2006;
70 Gunaseelaan et al., 2007 and 2009; Thomsen et al., 2014; Kafle et al., 2016). However, it
71 cannot be applicable to all OR as demonstrated by Mottet et al., (2010) who applied a Van
72 Soest fractionation to wastewater treatment sludge for BMP prediction. Bayard et al. (2015)
73 applied similar approach on agricultural and forest residues. Although the BMP and some

74 lignocellulosic characteristics of substrates were correlated, its prediction was low. Furthermore,
75 some of the results obtained concerning the impact of cellulose and hemicellulose on BMP
76 were contradictory (Thomsen et al., 2014). In the case of OR containing a mixture of all the
77 biochemical groups and a low fiber content, the first “Soluble” Van Soest fraction represented
78 more than 80% of VS (Mottet et al., 2010; Jimenez et al., 2015) and gathered a large diversity
79 of molecules that could not characterize the biodegradability. According to Lashermes et al.
80 (2009), Van Soest fractionation was not sufficient for the prediction of the IROC on a large
81 panel of residues. The addition of the organic carbon fraction mineralized after 3 days of
82 incubation can be associated to the readily biodegradable fraction which is generally high in
83 animal waste excluding litter and wastewater sludge.

84 Another common methodology for predicting BMP and carbon mineralisation on soil is Near
85 InfraRed Spectroscopy (NIRS). The use of the NIRS to quantify BMP (Lesteur et al., 2011;
86 Godin et al., 2015; Fitamo et al., 2017) has been successfully investigated, and subsequently
87 led to its commercial use at a later stage. A similar study was applied to the IROC (Peltre et
88 al., 2011). A few outliers were observed and mainly associated to wastewater sludge, liquid
89 manure and organo-mineral fertilisers. However, the NIRS method provides limited
90 qualitative information about chemical composition of OR due to overlapping overtones and
91 combination bands (Bekiaris et al., 2015b). This tool, therefore, does not facilitate a more
92 mechanistic interpretation.

93 More recently, a Fourier transform mid-infrared photoacoustic spectroscopy technique (FTIR-
94 PAS) was applied to predict BMP on plant biomass (Bekiaris et al., 2015a) and the
95 mineralisable fraction of carbon in soils from several OR (Bekiaris et al., 2015b). This
96 technique allowed for (i) the influence of sample particle size and absorption of dark and
97 opaque samples to be ignored and (ii) for more information to be produced on the
98 composition of OM than with NIRS (Bekiaris et al., 2015 a and b). In these two different

99 studies, although the authors demonstrated the impact of the composition of OR on
100 biodegradability prediction, they did not confront the results from both studies. Nonetheless,
101 differences and similarities did appear, as for example the ability of certain carboxylic acids to
102 produce both a negative effect on BMP on one hand, and a positive impact on mineralisable
103 soil carbon.

104 Few studies have dealt with anaerobic versus aerobic biodegradability correlations (Bayard et
105 al., 2015; Maynaud et al., 2017). However, no studies have yet focussed on the impact that
106 OM characterisation may have on both biodegradation pathways, and on the differences and
107 similarities between these impacts, in particular for BMP and soil incubation tests. Despite the
108 fact that some authors applied similar characterization tools for BMP test predictions in one
109 hand and soil carbon mineralization test on another hand, not a single study has yet addressed
110 the simultaneous prediction of both potentials.

111 Moreover, biodegradability of OR not only depends on the quantity of OM but it also relies
112 on the accessibility and complexity of the OM (Jimenez et al., 2015). Given the complex
113 organisation of certain organic residues, the term “accessibility” defines the potential access to
114 the molecules by microorganisms responsible for their degradation. It can depend on the
115 physical characteristics of the OR (particle size, porosity of the OR), on the distribution of the
116 organic fraction within the OR matrices in relation with the process duration, the hydrolytic
117 activity or the applied pre-treatment. Molecules with a weight below 1000 Da can pass through
118 the cell wall (Aquino, et al., 2008). Finally, once the OM becomes accessible, it can be more or
119 less easily biodegradable by microorganisms, depending on its chemical nature or complexity.

120 Cardeña et al. (2017) demonstrated that ozonation enhanced the accessibility of certain
121 microalgae which have structural and physical barrier to biodegradation, allowing, at the end,
122 their biodegradability. Furthermore, both complexity and accessibility have not yet been
123 considered together in any existing indicator. The chemical nature of extracted organic

124 fractions have been observed to vary during treatments such as composting, which thus
125 explains the change in biodegradability of given organic fractions (Peltre et al., 2012).
126 One study did successfully predict the biodegradability of sewage sludge under anaerobic
127 conditions by considering both accessibility and complexity (Jimenez et al., 2014). The
128 methodology developed was based on the combination of a sequential chemical extraction to
129 assess accessibility and fluorescence spectroscopy to assess the complexity of each extracted
130 organic fraction. Since, this sequential extraction methodology has been updated for
131 applications over a wider spectrum of OR (Jimenez et al., 2015). Maynaud et al. (2017) used
132 this combined approach in order to characterize solid and composted digestates. The authors
133 also performed anaerobic and aerobic tests without inoculum in order to characterize the
134 stability of the studied digestates. One main conclusion based on a statistical study
135 highlighted the strong potential of this methodology to predict digestate biodegradability.
136 According to the present literature review, the improvement of mechanistic knowledge and
137 optimisation of anaerobic digestion valorisation pathways are still limited by the lack of
138 studies dealing with the comparison between aerobic and anaerobic predictions from OM
139 characterisation. The updated methodology (Jimenez et al., 2015) has therefore been applied
140 to predict both anaerobic biodegradability thanks to BMP measurements and aerobic carbon
141 biodegradation in soil. The main objectives of this study are (i) to predict both energy
142 production and soil organic carbon potential using a combination of accessibility and
143 complexity characterisation performed on the same OR, (ii) to use the OM characterization to
144 analyse the similarities and differences between anaerobic biodegradability and soil organic
145 carbon mineralization and thus (iii) to identify OM characterization actuators in order to
146 optimize anaerobic digestion for methane production and organic amendments quality
147 requirements.

148 **Material and methods**

149 To assess the accessibility (i.e. sequential chemical extractions) and complexity (i.e.
150 fluorescence spectroscopy) of OM, eighty two OR were characterised with the recently
151 developed methodology. They were also incubated under anaerobic conditions during BMP
152 and 44 of them were incubated under aerobic conditions with crop soil. These incubation
153 tests led to the evaluation of the methane potential and potential residual organic carbon.
154 Statistical relations were investigated between the characterisation and the degradation
155 kinetics parameters.

156 a. Sample set

157 Eighty two samples were used for anaerobic incubation. The samples covered a large range of
158 types of OM. Indeed, the OR considered were: 2 biowastes (e.g. food waste); 3 Fermentable
159 Fractions of Municipal Solid Wastes (FFMSW) ; 3 green wastes, 4 initial composting
160 mixtures (2 sludge-green waste mixtures and 2 digested sludge-green waste mixtures), 22
161 composts (9 from sludge, 6 from digested sludge, 2 from biowaste digestates, 2 from FFMSW
162 digestates and 3 from manure digestates), 1 potting mix (e.g. commercial medium for plant
163 growth), 3 types of manure, 6 secondary wastewater sludge and 38 digestates obtained after
164 anaerobic digestion of sludge (11), manure (13), territorial waste mixtures (8), FFMSW (3)
165 and crop residues (3).

166 From these 82 samples used for anaerobic incubation, 44 samples were used for aerobic
167 incubation tests: these include 21 digestates (5 from sludge, 7 from manure, 3 from territorial
168 wastes, 3 from crop residues and 3 from FFMSW), 8 composts (4 from sludge digestates, 1
169 from manure digestate and 3 from sludge), 4 urban wastewater treatment sludge, 3 FFMSW, 3
170 manures, 2 green wastes, 2 initial composting mixtures (digested sludge and green waste
171 mixtures) and 1 potting mix. In addition, 3 samples were used for aerobic incubation only (i.e.
172 1 soil, 1 territorial waste, 1 crop residue digestate).

173 b. Physico-chemical characterization

174 The Dried Solids (DS) were analysed by gravimetry after 24h at 105°C and the Volatile
175 Solids (VS) were analysed by gravimetry after 2h at 550°C. The VS was obtained by
176 subtraction of the mineral matter obtained after 550°C and of the DS.

177 The Chemical Oxygen Demand (COD) was measured in duplicate using Aqualytic® kits (0-
178 1500 mg O₂.L⁻¹). Units were in mgO₂.L⁻¹ for the liquid phases and mgO₂.gDS⁻¹ for the solid
179 and total phases. Indeed, the analysis of the freeze-dried and grinded (1mm) sample was
180 performed on a solution of 1gDS.L⁻¹.

181 The Total Organic Carbon (TOC) was performed on grinded freeze-dried samples by
182 catalytic combustion at 900°C using a TOC-V-SSM-500A Shimadzu device. The units were
183 in mgC.gDS⁻¹.

184
185 c. Chemical fractionation

186 The application of a recently published method (Jimenez et al., 2015) was extended to a wider
187 range of organic residues. This methodology, based on chemical extractions that indicate the
188 chemical accessibility of organic residues, is a modified version of the protocol in (Jimenez et
189 al., 2014). The main modification consists in the addition of a sulfuric acid extraction step
190 from the Van Soest protocol (Van Soest, 1963) for determining the carbohydrates (i.e.
191 cellulose and hemicellulose). Sequential extractions (30 mL of each extractant) were
192 performed on 0.5-1 g of freeze-dried and grinded (1mm) samples. Each extraction stage was
193 followed by a centrifugation step (18600g, 20 minutes, 4°C) and a 0.45µm filtration step. The
194 resulting fractions were:

195 (1) Extractable Soluble from Particulate Organic Matter (SPOM) (milli-Q water solution
196 containing 10 mM of CaCl₂, 15 min × 4, 30°C, 300 rpm), which represents the most
197 accessible fraction and essentially contains water-soluble proteins and sugars.

198 (2) Readily Extractable Organic Matter (REOM) (NaOH 10 mM, 15 min × 4, 30°C, 300
199 rpm), which represents an accessible fraction of mainly proteins and lipids.

200 (3) Slowly Extractable Organic Matter (SEOM) (NaOH 0.1 M, 4 h × 4, 30°C, 300 rpm),
201 which mainly contains humic-like and fulvic-like acids and complex proteins (i.e. glycolated
202 proteins) as well as certain lignocellulosic compounds which can be soluble under strongly
203 basic conditions.

204 (4) Poorly Extractable Organic Matter (PEOM) (25 mL H₂SO₄, 72%, 3 h × 2, 30°C, 300
205 rpm), which targets holocelluloses (i.e. hemicellulose and cellulose).

206 (5) Non-Extractable Organic Matter (NEOM), which contains lignin-like compounds and
207 non-extractable humic-like acids (i.e. humin).

208 Results are expressed in COD (gO₂.gDS⁻¹).

209 d. 3D fluorescence spectroscopy

210 The acquisition of 3D fluorescence spectra was performed on the extracted fractions, allowing
211 for OM complexity to be qualified (Jimenez et al., 2014 and 2015). The complexity of OM
212 could be assessed through the proportions of fluorescence volumes of the most recalcitrant
213 molecules such as humic-like substances, fulvic-like acids, lipofuscin-like (i.e. a
214 lignocellulosic marker) as well as amino acids and less complex molecules (Muller et al.,
215 2014).

216 The fluorescence spectrometer was a Perkin Elmer LS55. Excitation wavelengths varied
217 between 200 and 600 nm with a 10 nm incrementation. Based on the work of Jimenez et al.
218 (2014) and Muller et al. (2014), spectra were decomposed into seven zones, each associated to
219 a particular biochemical family. The simplest molecules (i.e. amino acid fluorescence) are
220 located in zones 1 to 3 while the more complex molecules are located in zones 4 to 7. The

221 proportion of fluorescence for a given zone “i” $P_f(i)$ was calculated using the fluorescence
 222 zone volumes $V_f(i)$ according to Equations 1 and 2:

$$223 \quad V_f(i) (\text{U. A.}/\text{mg. COD. L}^{-1}) = \frac{V_{f,\text{raw}}(i)}{\text{COD}_{\text{sample}}} \times \frac{1}{\frac{S(i)}{\sum_{i=1}^7 S(i)}} \quad \text{Equation 1}$$

$$224 \quad P_f(i) (\%) = \frac{V_f(i)}{\sum_{i=1}^7 V_f(i)} \times 100 \quad \text{Equation 2}$$

225 with:

226

227 $V_f(i)$ (U.A. $\text{mg. O}_2 \cdot \text{L}^{-1}$): the normalized volume of the zone i,

228 $V_{f,\text{raw}}(i)$ (U.A. $\text{mg. O}_2 \cdot \text{L}^{-1}$): the raw volume of the zone i, $\text{COD}_{\text{sample}}$ ($\text{mg O}_2 \cdot \text{L}^{-1}$):
 229 the COD concentration of the sample,

230 $S(i)$ (nm^2): the area of a zone i,

231 $P_f(i)$ (%): the fluorescence proportion of a zone i.

232 e. Biodegradation tests

233 **Biochemical Methane Production (BMP) tests**

234 The BMP values were obtained using an innovative and rapid FlashBMP® method developed
 235 by Ondalys (Lesteur et al., 2011) and commercialized by Buchi. This method is based on
 236 Near InfraRed Spectroscopy (NIRS) applied to more than 600 types of OR (agro-industrial
 237 waste, green waste, energy crops, municipal solid waste, sludge and digestates) for which
 238 classical BMP tests were performed according to Angelidaki et al. (2004). Samples were
 239 freeze-dried and grinded to 1 mm before NIRS acquisition. Spectra were measured using a
 240 BUCHI NIRFlex N-500 (Buchi, Switzerland), with add-on vials, allowing for immediate
 241 analysis. Results are expressed in $\text{mL CH}_4 \cdot \text{gVS}^{-1}$.

242 **Soil incubation tests**

243 Freeze-dried and 1 mm grinded organic residues were incubated with 100 g of cropped soil,
244 (substrate: soil ratio between 0.002 and 0.01 g TOC product/g TOC dried soils) in
245 hermetically closed bottles (1L) during, at least 91 days under moisture and temperature
246 controlled conditions. For unlimited microbial growth conditions, mineral nitrogen was
247 added. Incubation of the soil without the addition of OR was also performed so as to take into
248 account the mineralization of soil organic carbon. The soil was provided by a control
249 treatment sampled during the QualiAgro field experiment (Ile de France, France) which began
250 in 1998 to study the effects of various organic fertilizers (Houot et al., 2002). Soil moisture
251 content was adjusted to a water content equivalent to 75 to 100% of the soil water holding
252 capacity. Carbon mineralization was monitored using a 20 mL trap solution of NaOH (0.5N)
253 for CO₂ which was periodically replaced during the incubations. The CO₂ was analysed by
254 titration of the remaining NaOH with HCl (1 M) or measured by gas chromatography (Perkin
255 Elmer CLARUS 480) following the acidification of the NaOH trap solution with HCl (1M) in
256 hermetic jars. Cumulated mineralized carbon was obtained as a percentage of initial TOC.
257 The mineralised TOC was identified as C_{bio} and results were expressed in gC.gC⁻¹.

259 **Statistical analysis**

260 In order to determine the correlations between biodegradability and indicators from OM
261 characterization, principal component analysis (PCA), hierarchical clustering analysis (HCA)
262 and partial least square (PLS) regressions were performed using SIMCA software from
263 UMETRICS.
264 In its simplest form, a linear model specifies the (linear) relationship between a dependent
265 (response) variable Y , and a set of X predictor variables, the X 's. The dataset was split into two
266 subsets: one for the calibration step (3/4 of the data) and one for the validation step (1/4 of the

267 data). Indeed, for the validation of the model set up to be robust, the dataset used for
268 calibration should not be the same as the dataset used for validation. In order to cover and
269 validate the whole range of data values, (i) the dataset was sorted by increasing the Y-variable
270 values and (ii) one out of four data points were selected for the validation step, as in Jimenez
271 et al. (2014).

272

273 The parameters from the PLS models used to assess model robustness are the following:

- 274 - Correlation coefficient R^2
- 275 - Root Mean Square Error (RMSE), used as an accuracy measurement of differences
276 between predicted values and measured model values.
- 277 - RMSEP is the RMSE for the prediction of validation samples
- 278 - Q^2 : percentage of variation of Y predicted by the PLS model according to cross-
279 validation. This parameter indicates how well the model predicts the data. A large Q^2
280 (>0.5) indicates good predictivity. Moreover, it is a compromise between root mean
281 square error and R^2 . Q^2 also represents the criteria for the choice of the component
282 number. In others words, when the cumulated Q^2 reaches its maximum value, the
283 corresponding component is selected.

284 **Results and discussion**

- 285 • Anaerobic biodegradability prediction

286 Based on the methodology of Jimenez et al. (2015), the 82 samples were first characterized
287 (fractionation and 3D fluorescence) and BMP measurements were performed. Samples
288 covered a large range of OM quality. Indeed, BMP values ranged from 31 to 394 Nml
289 $\text{CH}_4.\text{gVS}^{-1}$. The characterization data (X variables) were compared to the BMP data (Y
290 variable).

291 On one hand, PLS regression was applied using 33 explicative variables (X variables)
292 composed of $P_f(i)$ ($i= 1$ to 7), the fluorescence percentage of each zone and the COD percentage
293 of each fraction (e.g. SPOM, REOM, SEOM, PEOM, NEOM). This model is identified as
294 Model n°1. As suggested by Thomsen et al. (2014), the sum of the five fractions was equal to 1.
295 The residual non extractible OM (e.g. NEOM) was included in the PLS to remove
296 misinterpretations of regression coefficients weight due to relative nature of compositional data.
297 On another hand, Model n°2 was built using 5 explicative variables composed of the five
298 fractions. Out of the 82 observations, 56 were used to set up a first calibration for both
299 models. The validation samples were selected according to the increasing BMP values. One
300 sample out of four was used for validation (i.e. a total of 26 samples for validation).
301 Table 1 presents the quality parameters of the evaluated PLS models. Results clearly point out
302 that Model n°1 has the best prediction potential (i.e. $Q^2 = 0.689$ for Model 1 and 0.250 for model
303 2), highest correlation coefficient (i.e. $R^2 = 0.818$ for Model 1 and 0.410 for Model 2) and a low
304 RMSE value. The most significant and positive variables in Model 2 were the accessible SPOM
305 and REOM fractions. However, the lack of description in the quality fraction did not allow for
306 certain OR and OR digestates to be distinguished. Indeed, although some digestates had high
307 SPOM, they also contained non-biodegradable material that was not considered by fractionation
308 only. Consequently Model n°1 was selected. The quality of this model is illustrated in Figure 1.
309 The distribution of experimental Y-variables versus predicted Y-variables was similar to the
310 line of perfect fit ($y=x$) for BMP values. This result points to the closeness between the model
311 and experimental data. Three components were sufficient enough to explain 61% of the X-
312 variables (i.e. characterisation data) and 82% of the Y-variables (i.e. BMP data). The Root
313 Mean Square Error (RMSE) was $34 \text{ Nml CH}_4.\text{gVS}^{-1}$ and the Root Mean Square Error of
314 Prediction (RMSEP) was $66 \text{ Nml CH}_4.\text{gVS}^{-1}$. These results could allow for an accurate
315 prediction of the methane potential, with values ranging between 31 and 394 mL CH₄.gVS⁻¹.

316 According to the PLS scores and loading results (figures 2a, 2b, 2c), the BMP values were
317 positively correlated to the fluorescence zones 1 to 3 (i.e. protein-like compounds) and to the
318 SPOM fraction (i.e. the most accessible fraction). They were negatively correlated to the
319 SEOM fraction and to the complex fluorescence zones (4 to 7) from all fractions. Therefore, the
320 first component was essentially characterised by the complexity of the OR (figure 2b), the
321 second component was characterised by the SPOM fraction, while the third one was negatively
322 correlated to the SEOM (figure 2c) and positively correlated to the SPOM. Finally, these second
323 and third components were rather related to the OR accessibility.

324 Table 2 highlights the impact of the most significant X-variables affecting the prediction of
325 Y-variables derived from the calculation of the weight of each variable. Positive and
326 significant variables comprised the SPOM fraction and the fluorescence zone 3 related to
327 protein-like molecules from all organic fractions. Bayard et al. (2015) observed similar
328 results with good correlations between BMP values and water soluble COD applied on
329 biowastes, residual municipal solid waste and their digestates. Moreover, with the use of
330 principal component analysis, Maynaud et al. (2017), pointed out that SPOM and
331 fluorescence zones 1 to 3 were correlated with BMP values of digestates.

332 Conversely, the negative and significant variables were associated to the SEOM fraction (i.e.
333 the moderately accessible fraction) and to the complex fluorescence zones 4 and 6 from
334 REOM, related to complex molecules such as humic-like and fulvic-like acids. Bayard et al.
335 (2015) also demonstrated that the humic substance index (i.e. obtained using a similar NaOH
336 extraction as for SEOM followed by an acid precipitation to recover fulvic acids) had a
337 negative impact on BMP values of biowastes and their digestates.

338 This result implies that the combination of accessibility and fluorescence-derived complexity
339 could allow for the prediction of organic residue biodegradability under anaerobic conditions.

340 A Hierarchical Clustering Analysis (HCA) was performed simultaneously with the PLS. This
341 analysis highlighted 6 observation groups, as illustrated by the scores plot in Figure 2a.
342 According to this analysis, the highest BMP values are positively correlated to the fluorescence
343 zones 1 to 3 (i.e. protein-like) and to the SPOM fraction (i.e. the most accessible fraction).
344 They are associated with Group n°4 samples that are mainly composed of sludge, biowaste and
345 vegetables (e.g. potatoes). Conversely, the lowest BMP values are negatively correlated to the
346 complex fluorescence zones (4 to 7). They are associated with Groups n°1 and 2, according to
347 their content in accessible fractions and are essentially composed of well stabilized
348 manure/territorial digestates and biowaste/FFMSW composts, digestate composts and potting
349 mix. These results are consistent: the more the OR are complex and poorly accessible, the
350 lower the biodegradability. In terms of BMP, intermediate groups could be formed: Group 5
351 mainly contains digestates with high SEOM fractions (sludge and manure) while Group 6 is
352 mainly composed of FFMSW, manure and lignocellulose-like compounds with higher BMP
353 than the digestate groups. Group 3, comprising two samples (sludge compost and initial
354 mixture between green waste and digestate sludge), is close to the rich SEOM Group n°5.
355 Jimenez et al. (2015) demonstrated that this characterisation, based on the two concepts of
356 accessibility and complexity, could help to categorise organic residues. Indeed, this study
357 confirms that the anaerobic biodegradability of a large panel of OR can be concurrently
358 categorized and predicted thanks to this methodology.

359 • Prediction of organic carbon biodegradability

360 As for BMP prediction, the correlation between OR characteristics and aerobic mineralisation
361 results was investigated thanks to a PLS regression using the same 33 explicative variables as
362 for BMP (i.e. Model n°3), and using the 5 fractions (i.e. Model n°4). A first calibration model
363 was set-up for 31 observations and 16 samples were used for validation, in the same manner
364 as for BMP prediction.

365 The Y-variable was the aerobic carbon biodegradability (C_{bio}) fraction of TOC measured
366 during soil incubation tests. The dataset was obtained from a huge diversity of organic
367 residues with a high range of biodegradability (from 7 to 46 % TOC).

368 From table 1, results implied that the Model n°3 had the best prediction quality (Q² = 0.745 for
369 Model 3 and 0.456 for Model 4), a high correlation coefficient (R² = 0.845 for Model 3 and
370 0.632 for Model 4) and a low RMSE value. The most significant variables in Model 4 include
371 the accessible fraction REOM (positively correlated) and NEOM (negatively correlated).
372 Despite the promising prediction potential of Model 4, the poor quality description of the
373 fraction did not allow for certain OR (i.e. sludge and manure) and their respective digestates to
374 be distinguished as for BMP prediction. Consequently, Model n°3 was selected for C_{bio}
375 prediction.

376 As illustrated by Figure 3, the plot of measured values versus predicted values points to the
377 ability of this model to predict biodegradable organic carbon (i.e. closest to the perfect fit
378 line). Two components were required to explain 53% of X-variables. The RMSE accounted
379 for 5.1% of TOC while the RMSEP accounted for 7.3% of TOC.

380 The scores and loadings of the PLS model are plotted in Figure 4. According to this plot, the
381 first component is defined by the fluorescence-derived complexity, while the second
382 component is defined by the accessibility axis. Indeed, as for BMP prediction, C_{bio} was
383 positively impacted by the most accessible fraction SPOM and by the simplest fluorescence
384 zones represented by the protein-like in SPOM and REOM. Conversely, the least accessible
385 fraction NEOM was negatively related to the organic carbon mineralisation. This is contrary
386 to the BMP model for which NEOM was not significant. However, again as for BMP
387 prediction, the most complex fluorescence zones of the 3D fluorescence spectra of SPOM and
388 REOM represented by humic-like, fulvic-like acids and lignocellulose-like molecules also had
389 a strong negative impact on carbon mineralization.

390 The HCA comprised 6 groups of observations, as presented by the scores in Figure 4. Group
391 n°1 was mainly composed of sludge and sludge digestate and characterised by the highest
392 C_{bio} values. Sludge samples were characterised by a large REOM fraction and the simplest
393 fluorescence zones from REOM and SPOM while, similarly to BMP prediction, sludge
394 digestates were rather characterised by a large SEOM fraction. Nevertheless, sludge digestate
395 was part of a separate group in BMP prediction and not part of the same group as for C_{bio}
396 (i.e. the most biodegradable samples). This confirms that, depending on their OM
397 characteristics, aerobic and anaerobic biodegradation potentials cannot be similar for all
398 substrates. Some digestates could be more biodegradable under aerobic soil incubation than in
399 anaerobic BMP tests. In contrast, similarly to the soil and to the potting mix, Group n°4
400 contained the poorest biodegradable OR. They were characterised by a high NEOM fraction
401 and complex fractions of SPOM. This latter characteristic was also observed in the group
402 characterised by low BMP values (i.e. potting mix, close to stabilized composts).

403 Other groups were categorised as intermediate according to their nature. Indeed, Group n°2
404 was composed of FFMSW, initial composting mixtures of green waste and sludge, and
405 vegetables, which represented a mixture of compounds that were rich in either protein-like
406 fractions, or lignocellulose-like fractions. Group n°3 was composed of digestates from
407 territorial OR or from crop residues. They were associated to a large PEOM fraction and to
408 complex fluorescence zones in this fraction. Groups n° 5 and 6 contained manure digestates,
409 wooden structures and composts in the lower part (rather associated with a high NEOM
410 fraction and manure, i.e. a lignin-like content), and FFMSW digestates and green waste in the
411 upper part (mainly associated with a large PEOM fraction, i.e. a cellulose and hemicellulose
412 content). All these samples were also characterised by complex fluorescence zones from
413 PEOM fraction.

414 As for the BMP prediction model, Table 2 highlights the impact of the most significant X-
415 variables on the Y-variable prediction and confirms all the previous observations. Concerning
416 the prediction of C_{bio}, the most significant positive variables were PEOM, SPOM, REOM
417 and SEOM with fluorescence zones 1 to 3 (i.e. protein-like) from SPOM and REOM and
418 fluorescence zones 5 and 6 from SEOM. The most significant negative variables were NEOM
419 and certain complex fluorescence zones from SPOM and REOM.

420

421 • Anaerobic versus soil aerobic biodegradability: impact of OM quality

422 In Table 2, the weight of the model variables revealed existing similarities and differences
423 between anaerobic biodegradability and aerobic soil incubation. Both types of
424 biodegradability were positively impacted by the SPOM fraction and the simplest
425 fluorescence zones.

426 However, contrary to the BMP value prediction, SEOM showed a positive influence on
427 aerobic biodegradability, namely its fluorescence zones 5 and 6. Indeed, the SEOM fraction
428 and its fluorescence zone 6 were related to humic-like substances, which are mostly found in
429 digestates. This fraction and the associated molecules which tend to be recalcitrant under
430 anaerobic conditions showed a positive influence in soil incubation conditions. This is
431 consistent with the nature of the molecules which can affect the production of humus.
432 Consequently, combining anaerobic digestion (by optimising the anaerobic recalcitrant
433 SEOM-like production) with the digestate landspreading could entail a higher organic
434 fertilizing value. Digestate characterisation results from a statistical analysis of nuclear
435 magnetic resonance data (Tambone et al., 2010), showed how anaerobic digestion is capable
436 of preserving recalcitrant molecules (i.e. lignin-like, steroids or complex lipids) known as
437 humus precursors.

438 The PEOM and NEOM fractions presented a significant impact on C_{bio} predictions while
439 these same fractions had no significant effect on BMP. This is consistent with the results
440 obtained by Lashermes et al. (2009) involving a positive impact of the cellulose fraction and a
441 negative impact of the lignin fraction, both being obtained by Van Soest fractionation.

442 Moreover, even though the most biodegradable samples contain a large fraction of SPOM and
443 a high content of protein-like fluorescence zones, aerobic biodegradation appears to be further
444 advanced than anaerobic biodegradation. In both cases, the characterisation protocol was
445 sufficiently detailed for both mineralization potentials to be predicted. In addition, the
446 differences between both pathways could lead to a balance between methane and organic
447 amendment production. For example, sludge digestates and certain manure digestates that are
448 rich in the moderately accessible SEOM fraction, presented high C_{bio} values. These are
449 more appropriate for fertility purposes while NEOM-rich digestate composts and complex
450 molecules with low C_{bio} values should be more appropriate for long-term organic
451 amendment.

452 Characterisation data used in common for both models (e.g. BMP and aerobic soil
453 biodegradation) have been used to investigate the correlations between the BMP and C_{bio}
454 variables. Figure 5 illustrates the resulting correlation. C_{bio} and BMP were positively and
455 significantly correlated, with a Pearson coefficient of R= 0.787. In addition, a linear
456 regression between BMP and C_{bio} data was established with the following equation: $BMP =$
457 $474.98 \times C_{bio} + 15.462$, with a correlation coefficient of $R^2 = 0.619$, meaning that only 62%
458 of the samples variance is explained by the linear regression.

459 In some cases, two samples had similar BMP values but very different and lower C_{bio}
460 values (for example this could be the case for green waste and sludge; potting mix and
461 territorial digestate). Despite the fact that, in many cases, the biodegradable state of OM is

462 generally stable under both anaerobic and aerobic conditions, the structural and functional
463 diversity of soil microbial communities tend to enhance OM degradation under aerobic
464 conditions.

465 In the literature, many authors have tried to correlate BMP test values with rapid aerobic test
466 results (i.e. respirometry). They observed reliable and positive correlations between these two
467 tests that were performed on the same types of organic residues. Cossu et al. (2008) and
468 Scaglia et al., (2010) found such correlations on MSW landfill ($R^2 > 0.80$ and 0.89
469 respectively); positive correlations between BMP and Biological Oxygen Demand tests were
470 also observed by Liu et al. (2015) with agricultural and forest residues ($R^2 > 0.94$) and Bayard
471 et al. (2015) with biowaste and digested biowaste ($R^2 = 0.81$). Maynaud et al. (2017) also
472 demonstrated a good correlation between anaerobic biodegradability and aerobic
473 biodegradability obtained on solid and composted digestates without inoculum addition ($R^2 =$
474 0.8). In the present work, aerobic biodegradability is achieved by soil incubation. This main
475 difference with other studies reported from the literature suggests that aerobic inoculum from
476 soil was completely different in terms of diversity and biodegradation ability.

477 As previously mentioned, the organic carbon stability and potential efficiency of increasing
478 soil OM were usually estimated with the IROC calculated as a function of the fractions
479 provided by the Van Soest methodology and a 3-day carbon mineralisation test (C3d)
480 (Lashermes et al., 2009). According to the authors, the models built with the Van Soest
481 fractionation variables were not sufficiently robust and accurate to predict the IROC whereas
482 the addition of the C3d favoured a better prediction. The C3d variable was the most
483 significant variable of the IROC model, positively correlated with biodegradable TOC and
484 associated with the most readily biodegradable OR (i.e. sludge, liquid manure, animal wastes
485 without litter). Besides, the soluble fraction used for the IROC calculation is positively
486 correlated to the residual TOC obtained at the end of the incubation (Lashermes et al., 2009).

487 This soluble fraction is very large for a lot of protein-like OR (i.e. sludge, liquid manure,
488 some animal wastes, digestates) according to Lashermes et al. (2009), Mottet et al. (2010),
489 Peltre et al. (2011), and Jimenez et al. (2015). Despite its accessible chemical feature, this
490 fraction can contain both biodegradable and non-biodegradable molecules (Peltre et al.,
491 2011). Prediction of biodegradable TOC still needs to be improved due to a lack in
492 complexity information. Moreover, in contrast to the fractionation procedure applied in this
493 study, the humic-like fraction was absent in the Van Soest fractionation. Indeed, thanks to the
494 SEOM fraction and 3D fluorescence spectroscopy, it is possible to identify and include
495 humification in organic waste characterisation. According to the type of sample, the SEOM
496 fraction contains mainly complex protein-like molecules or/and humic-like substances
497 (Jimenez et al., 2015). Also, the fluorescence signal of this fraction reveals the degree of
498 complexity which can then be associated to its biodegradability. As PLS models have proved,
499 the SEOM fraction represents a key variable for both soil carbon mineralization and BMP
500 predictions. Humification, being a key process in organic carbon stabilisation, could account
501 for a more efficient capacity in increasing soil organic carbon stocks after spreading. Unlike
502 the IROC indicator, this methodology has the capacity to better take into account the chemical
503 nature of the extracted fractions and their evolution during treatment for the prediction of the
504 potential efficiency of increasing soil organic matter after residue application. The same OM
505 fractionation combined with 3D-fluorescence spectroscopy has enabled the prediction of both
506 methane production and mineralisable soil carbon: these input variables could be used in
507 future investigations to combine dynamic models of carbon fate in conditions ranging from
508 anaerobic digestion to soils. Results have shown how anaerobic digestion and soil incubation
509 can be complementary regarding OM biodegradability for methane production and OM
510 stability for soil amendment purposes. Depending on the soil constraints, this approach is a
511 first step in optimising the whole processing chain from anaerobic digestion to soils.

512 Indeed, the main issue for this kind of modelling is the difference between the considered
513 input/output variables of the models (ADM1, Batstone et al., 2002; Garnier et al., 2003; Sole-
514 Mauri et al., 2007; Oudart et al. 2012; Zhang et al. 2012; Denès 2015). The next step should
515 be to use these fractions as common variables in mechanistic models in order to simulate OM
516 accessibility throughout the whole processing chain of OR until soil utilisation.

517 **Conclusions**

518 Chemical accessibility and fluorescence spectroscopy have proved to predict both methane
519 potentials and soil mineralized carbon, implying that the methodology can be used for aerobic
520 and anaerobic decomposition models if plant-wide modelling is considered. Moreover,
521 humic-like acids fraction and its associated fluorescence zone appeared to be recalcitrant for
522 BMP but positive for C_{bio} prediction. These differences could be used as actuators since
523 these recalcitrant molecules can be precursors of humus production, thus promoting the
524 choice of digestate spreading. It is the first step towards improving the quality control of OR
525 for their valorisation to be most profitable.

526 **Acknowledgements**

527 The authors want to acknowledge the ADEME (PROLAB project n°1306C0055 and
528 PROBIOTIC project) and ONEMA (Risq-PRO project, action 12-5-1) for their financial
529 support.

530 **References**

- 531 1. Angelidaki, I. and Sanders, W. (2004) Assessment of the anaerobic
532 biodegradability of macropollutants. *Reviews in Environmental Science and*
533 *Bio/Technology* 3, 117-129.

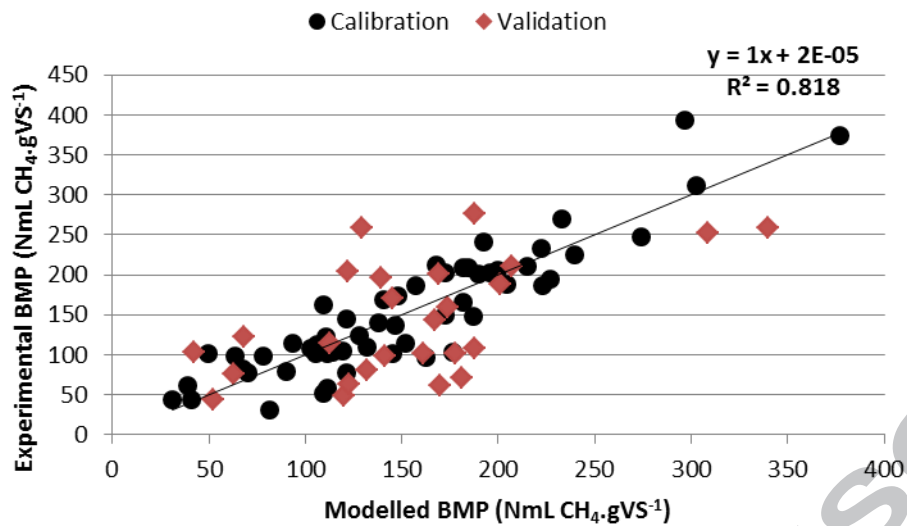
- 534 2. Batstone, D. J., Keller, J., Angelidaki, I., Kalyuzhnyi, S. V., Pavlostathis, S. G., Rozzi,
535 A., Sanders, W. T. M., Siegrist, H., Vavilin, V. A. (2002) Anaerobic Digestion Model
536 No.1. (ADM1). IWA Scientific and Technical Report No. 13. IWA, ISBN:1-900222-
537 78-7.
- 538 3. Bayard, R., Gonzalez-Ramirez, L., Guendouz, J., Benbelkacem, H., Buffiere, P.,
539 Gourdon, R., (2015) Statistical analysis to correlate bio-physical and chemical
540 characteristics of organic wastes and digestates to their anaerobic biodegradability.
541 Waste Biomass Valor. 6 (5), 759–769.
- 542 4. Bekiaris, G., Triolo, J. M., Peltre, C., Pedersen, L., Jensen, L. S., and Bruun, S. (2015a)
543 Rapid estimation of the biochemical methane potential of plant biomasses using Fourier
544 transform mid-infrared photoacoustic spectroscopy. Bioresource Technology, 197,
545 475–481.
- 546 5. Bekiaris, G., Bruun, S., Peltre, C., Houot, S., and Jensen, L. S. (2015b) FTIR–PAS: A
547 powerful tool for characterising the chemical composition and predicting the labile C
548 fraction of various organic waste products. Waste Management, 39, 45–56.
- 549 6. Buffiere, P., Loisel, D., Bernet, N. and Delgenes, J. P. (2006) Towards new
550 indicators for the prediction of solid waste AD properties. Water Science and
551 Technology 53 (8), 233-241.
- 552 7. Cardeña, R., Moreno, G., Bakonyi, P., Buitrón, G. (2017) Enhancement of methane
553 production from various microalgae cultures via novel ozonation pretreatment.
554 Chemical Engineering Journal, 307, 948-954.
- 555 8. Gunaseelan, V. N. (2007) Regression models of ultimate methane yields of
556 fruits and vegetables solid wastes, sorghum and napiergrass on chemical
557 composition. Bioresource Technology 98, 1270-1277.

- 558 9. Gunaseelan, V. N. (2009) Predicting ultimate methane yields of *Jatropha curcus* and
559 *Morus indica* from their chemical composition. *Bioresource Technology* 100 (13),
560 3426-3429.
- 561 10. Houot S., Clergeot D., Michelin J., Francou C., Caria G. and Ciesielski H. (2002)
562 Agronomic value and environmental impacts of urban composts used in agriculture.
563 In "Microbiology of composting" H.Insam, N. Riddech and S. Klammer Eds,
564 Springer-Verlag, Berlin Heidelberg, 457-472.
- 565 11. Cossu, R., Raga, R. (2008) Test methods for assessing the biological stability of
566 biodegradable waste. *Waste Management*, 28 (2) 381-388.
- 567 12. Denes, J., Tremier, A. , Menasseri-Aubry, S., Walter, C., Gratteau, L., Barrington, S.
568 (2015) Numerical simulation of organic waste aerobic biodegradation: A new way to
569 correlate respiration kinetics and organic matter fractionation. *Waste Management*,
570 36, 44-56.
- 571 13. Fitamo, T., Triolo, J. M., Boldrin, A., and Scheutz, C. (2017) Rapid biochemical
572 methane potential prediction of urban organic waste with near-infrared reflectance
573 spectroscopy. *Water Research*.
- 574 14. Garnier, P., Neel C., Aita, C., Recous, S., Lafolie, F., Mary, B., (2003) Modelling
575 carbon and nitrogen dynamics in a bare soil with and without straw incorporation.
576 *European journal of soil science*, 54, 555-568.
- 577 15. Godin, B., Mayer, F., Agneessens, R., Gerin, P., Dardenne, P., Delfosse, P., and
578 Delcarte, J. (2015) Biochemical methane potential prediction of plant biomasses:
579 Comparing chemical composition versus near infrared methods and linear versus
580 non-linear models. *Bioresource Technology*, 175, 382–390.
- 581 16. Jimenez, J., Gonidec, E., Cacho Rivero, J.A., Latrille, E., Vedrenne, F., Steyer, J.-P.
582 (2014) Prediction of anaerobic biodegradability and bioaccessibility of municipal

- 583 sludge by coupling sequential extractions with fluorescence spectroscopy: towards
584 ADM1 variables characterization. *Water Res.*, 50, 359–72.
- 585 17. Jimenez, J., Aemig, Q., Doussiet, N., Feurgard, I., Steyer, J.-P., Patureau, D., Houot,
586 S. (2015) Towards a unified organic waste characterization of organic matter
587 accessibility and complexity. *Bioresource Technology*, 194, 344-353.
- 588 18. Kafle, G. K. and Chen, L. (2016) Comparison on batch anaerobic digestion of five
589 different livestock manures and prediction of biochemical methane potential (BMP)
590 using different statistical models. *Waste Management*, 48, 492–502.
- 591 19. Lashermes, G., Nicolardot, B., Parnaudeau, V., Thuriès, L., Chaussod, R., Guillotin,
592 M.L., Linères, M., Mary, B., Metzger, L., Morvan, T., Tricaud, A., Villette, C.,
593 Houot, S. (2009) Indicator of potential residual carbon in soils after exogenous
594 organic matter application. *European Journal of Soil Science*, 60, 297–310.
- 595 20. Lesteur, M., Latrille, E., Maurel, V. B., Roger, J. M., Gonzalez, C., Junqua, G. and
596 Steyer, J. P. (2011) First step towards a fast analytical method for the
597 determination of Biochemical Methane Potential of solid wastes by near infrared
598 spectroscopy. *Bioresource Technology*, 102 (3), 2280-2288.
- 599 21. Liu, X., Bayard, R., Benbelkacem, H., Buffière, P., Gourdon, R. (2015) Evaluation
600 of the correlations between biodegradability of lignocellulosic feedstocks in
601 anaerobic digestion process and their biochemical characteristics. *Biomass and*
602 *Bioenergy*, 81, 534-543.
- 603 22. Mottet, A., François, E., Latrille, E., Steyer, J.P., Déléris, S., Vedrenne, F., Carrère,
604 H. (2010) Estimating anaerobic biodegradability indicators for waste activated
605 sludge. *Chem. Eng. J.*, 160, 488–496.
- 606 23. Maynaud G., Druilhe C., Daumoin, M., Jimenez J., Patureau, D., Torrijos M., Pourcher
607 AM., Wery, N. (2017) Characterisation of the biodegradability of post-treated

- 608 digestates via the chemical accessibility and complexity of organic matter. *Bioresource*
609 *and Technology* 231, 65-74.
- 610 24. Parnaudeau, V., Nicolardot, B., Robert, P., Alavoine, G., Pagès, J., Duchiron, F.
611 (2006) Organic matter characteristics of food processing industry wastewaters
612 affecting their C and N mineralization in soil incubation. *Bioresource Technology*,
613 97 (11), 1284-1295.
- 614 25. Oudart, D., Paul, E., Robin, P., Paillat, J.M. (2012) Modeling organic matter
615 stabilization during windrow composting of livestock effluents. *Environmental*
616 *Technology*, 33(19), 2235-2243.
- 617 26. Peltre C., Dignac M.F., Derenne S., Houot S. (2010) Change of the chemical
618 composition and biodegradability of the Van Soest soluble fraction during
619 composting: A study using a novel extraction method. *Waste Management*, 30(12),
620 2448-2460.
- 621 27. Peltre C., Thuriès, L., Barthès, B., Brunet, D., Morvan, T., Nicolardot, B.,
622 Parnaudeau, S., Houot S. (2011) Near infrared reflectance spectroscopy: A tool to
623 characterize the composition of different types of exogenous organic matter and their
624 behaviour in soil. *Soil Biology and Biochemistry*, 43, 197-205.
- 625 28. Peltre C., Christensen B.T., Dragon S., Icard C., Kätterer T., Houot S. (2012) RothC
626 simulation of carbon accumulation in soil after repeated application of widely
627 different organic amendments. *Soil Biology and Biochemistry*, 52, 49-60.
- 628 29. Ponsá, S., Gea, T., Alerm, L., Cerezo, J., Sánchez, A., (2008) Comparison of aerobic
629 and anaerobic stability indices through a MSW biological treatment process. *Waste*
630 *Management* 28 (12), 2735–2742.

- 631 30. Scaglia, B., Confalonieri, R., D'Imporzano, G., Adani, F. (2010) Estimating biogas
632 production of biologically treated municipal solid waste. *Bioresource*
633 *Technology*, 101 (3), 945-952.
- 634 31. Sole-Mauri, F., Illa, J., Magrí, A., Prenafeta-Boldú, F. X., Flotats, X. (2007) An
635 integrated biochemical and physical model for the composting process. *Bioresource*
636 *Technology*, 98 (17), 3278-3293.
- 637 32. Tambone, F., Scaglia, B., D'Imporzano, G., Schievano, A., Orzi, V., Salati, S., Adani,
638 F., (2010) Assessing amendment and fertilizing properties of digestates from anaerobic
639 digestion through a comparative study with digested sludge and compost. *Chemosphere*
640 81 (5), 577-83.
- 641 33. Thomsen, S. T., Spliid, H., and Østergård, H. (2014) Statistical prediction of
642 biomethane potentials based on the composition of lignocellulosic biomass.
643 *Bioresource technology*, 154, 80-6.
- 644 34. Van Soest, P. J. (1963) Use of detergents in the analysis of fibrous feeds. II. A rapid
645 method for the determination of fiber and lignin. *Journal of the Association of*
646 *Official Analytical Chemists* 46, 829-835.
- 647 35. Zhang, Y., Lashermes, G., Houot, S., Doublet, J., Steyer, J.P., Zhu, Y.G., Barriuso, E.,
648 Garnier, P., (2012) Modelling of organic matter dynamics during the composting
649 process. *Waste Manag.* 32, 19-30.
- 650
- 651



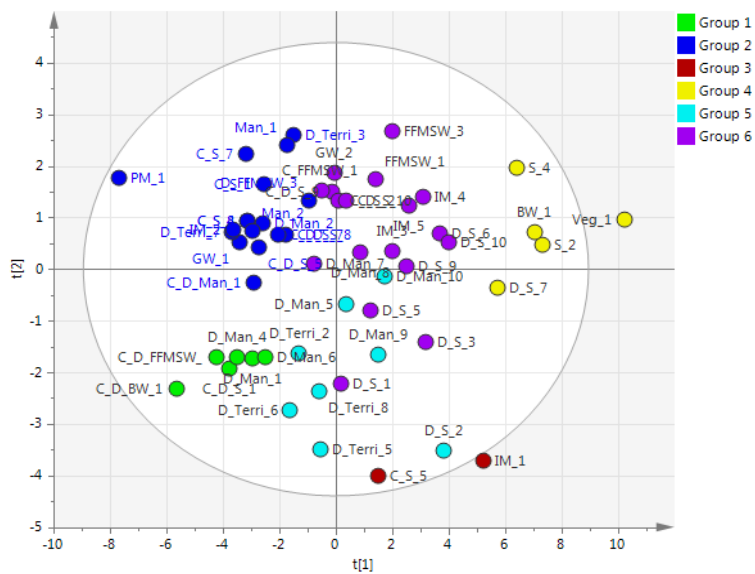
652

653 Figure 1: Observed versus predicted BMP value obtained with the PLS model n°1 (black dots: calibration data and red dots:

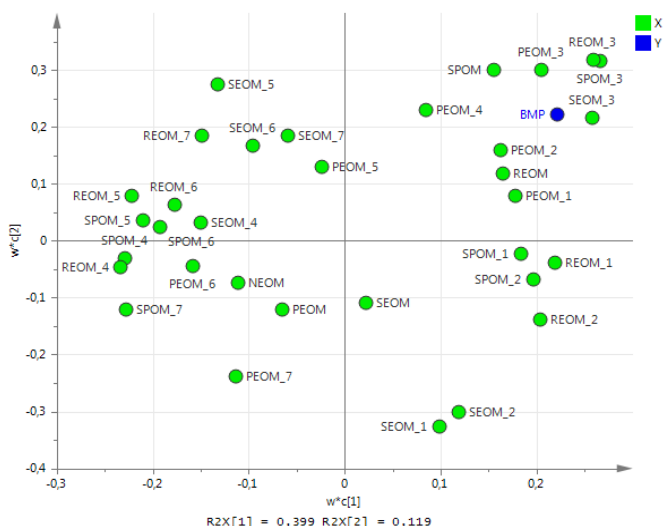
654 validation data)

655

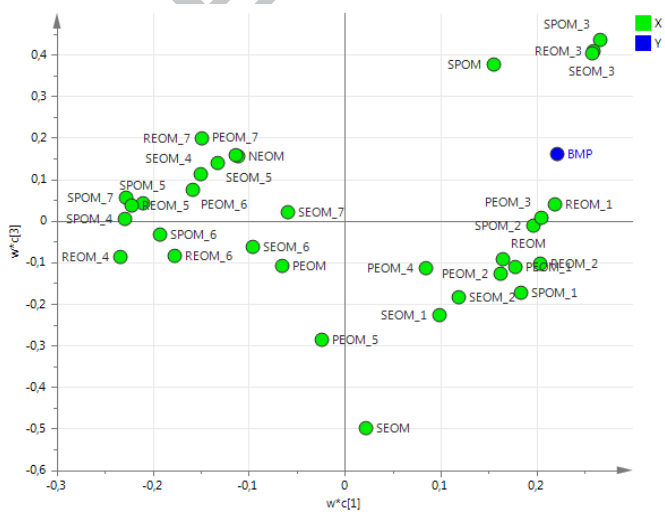
656



657 $\lambda = 0,399$ $R^2X[2] = 0,119$ Ellipse: Hotelling's T2 (95%) (a)



658 $R^2X[1] = 0,399$ $R^2X[2] = 0,119$ (b)



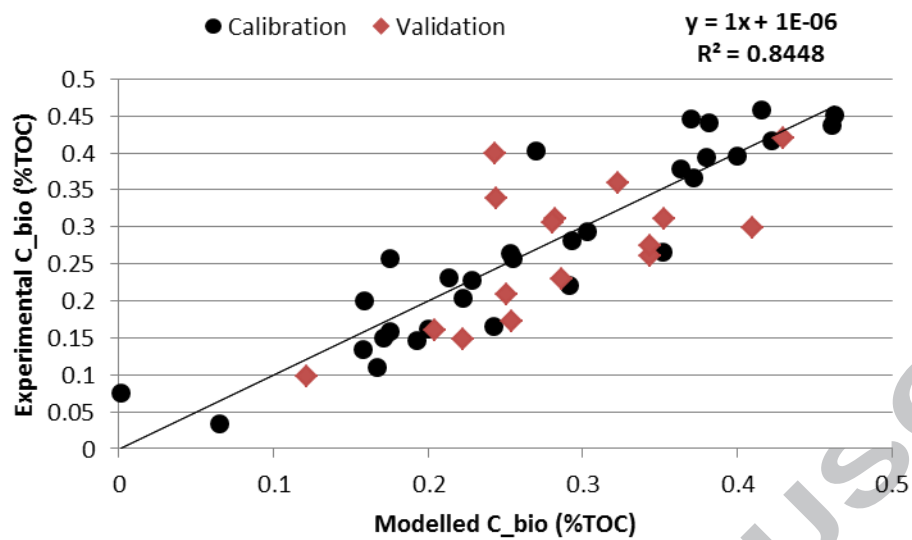
659 $R^2X[1] = 0,399$ $R^2X[3] = 0,0905$ (c)

660 Figure 2: Scores obtained on calibration data and HCA analysis (a) and loadings plots (b) and (c) for BMP prediction model n°1

661

ACCEPTED MANUSCRIPT

663



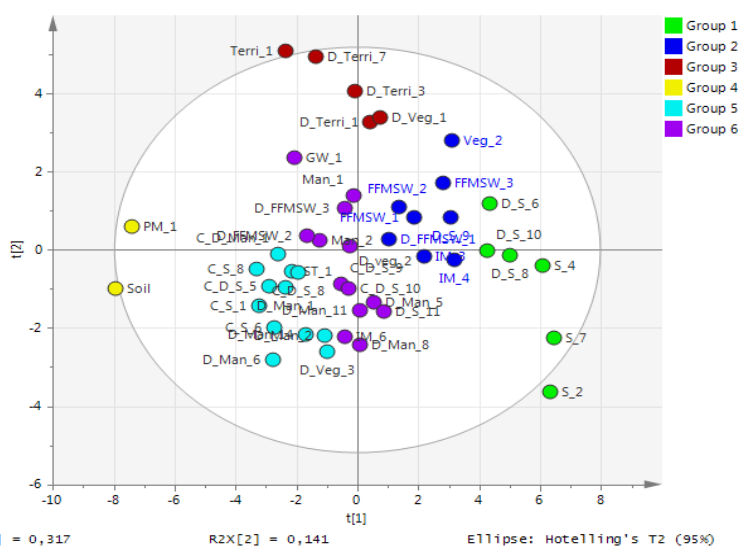
664

665 Figure 3: Observed versus predicted C_{bio} value obtained with the PLS model n°3 (black dots: calibration data and red dots:
666 validation data)

667

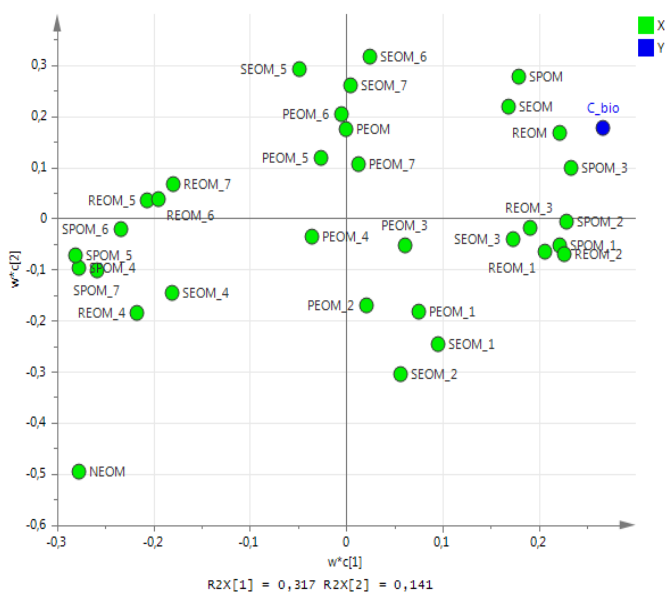
668

669



670

(a)



(b)

671

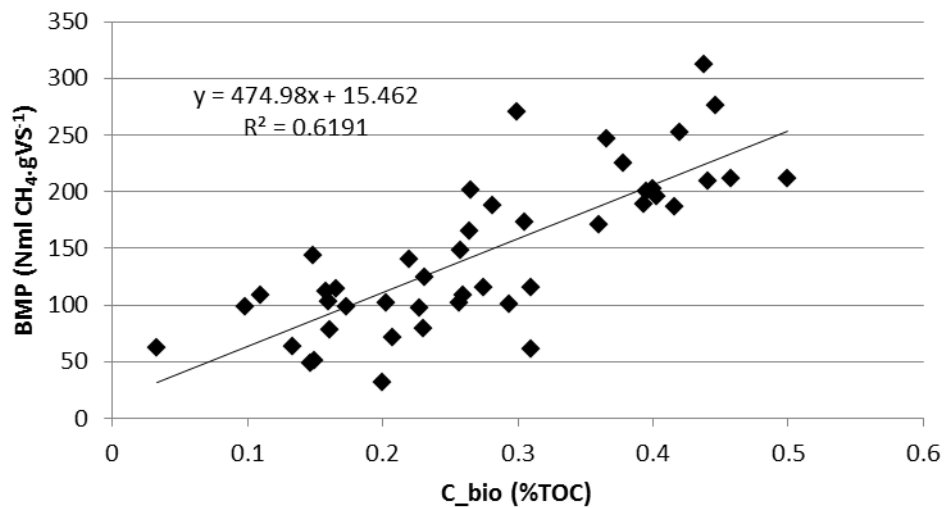
672 Figure 4: Scores (a) and loadings (b) related to the C_{bio} variable prediction applied on all the data

673

674

675

676



677

678 Figure 5: Correlation between BMP experimental values and C_bio experimental values

679

680

681 Table 1: Quality parameters of the PLS models for BMP and C_{bio} prediction

Y-Variables	X-variables	Model	Number of Component	RMSE	RMSEP	R ² X	R ² Y	R ² Y (calibration+validation)	Q ²
BMP (NmICH₄.gVS⁻¹)	33 (fractions and fluorescence data)	1	3	33.950	65.788	0.608	0.818	0.637	0.689
BMP (NmICH₄.gVS⁻¹)	5 (fractions)	2	2	60.542	61.599	0.583	0.41	0.366	0.250
C_{bio} (%COT)	33 (fractions and fluorescence data)	3	2	0.051	0.073	0.528	0.845	0.738	0.745
C_{bio} (%COT)	5 (fractions)	4	2	0.078	0.098	0.58	0.632	0.549	0.456

682

683

684 Table 2: Significant positive and negative impacts of the X-variables on Y-variables prediction obtained from coefficients

685 weight and variable importance for projection plots

X-Variables\Y-Variables	BMP	C _{bio}
S POM	+++	+
Fluorescence Zones 1-3	+++	++
Fluorescence Zones 4-7	0	--
REOM	0	+
Fluorescence Zones 1-3	+++	+
Fluorescence Zones 4-7	-	--
SEOM	--	+
Fluorescence Zones 1-3	+++	0
Fluorescence Zones 4-7	0	+
PEOM	0	++
Fluorescence Zones 1-3	++	0
Fluorescence Zones 4-7	0	0
NEOM	0	---

686 Legend:

687 +: positive impact; -: negative impact

688 +++/---: extremely sensitive (weight >0.15); +/-/: very sensitive (0.1<weight<0.15); +/-/: sensitive (0.05<weight<0.1); 0: not sensitive;

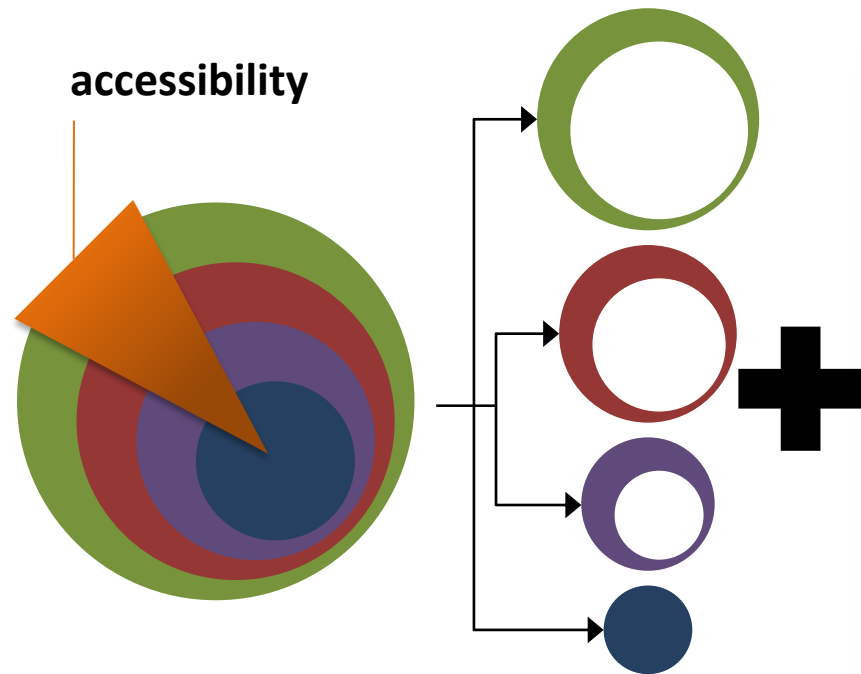
689

690

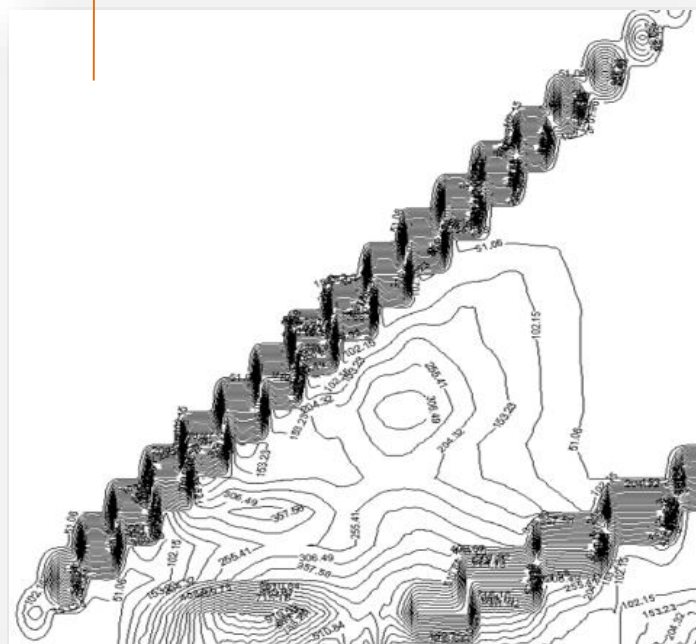
691 **Highlights**

- 692 •Fractionation and fluorescence data allowed the best prediction of biodegradability.
- 693 •Differences and similarities are observed on the variables impact on predictions.
- 694 •Humic-like fraction has a negative impact on BMP but not on soil mineralized carbon.
- 695 •Actuators identification can be found to control valorization ways.

696



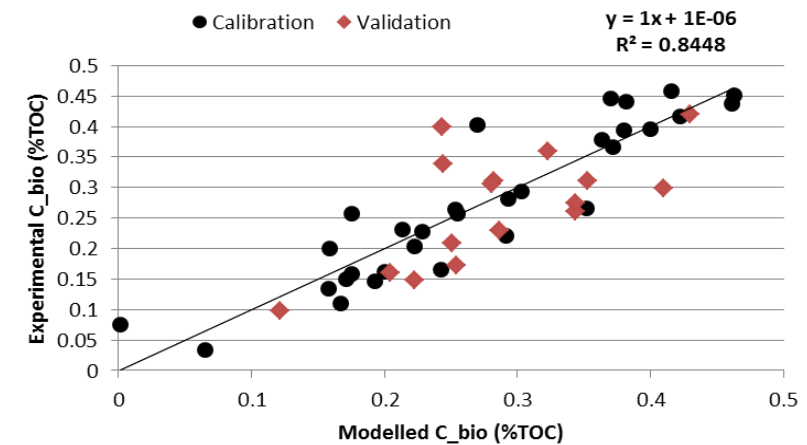
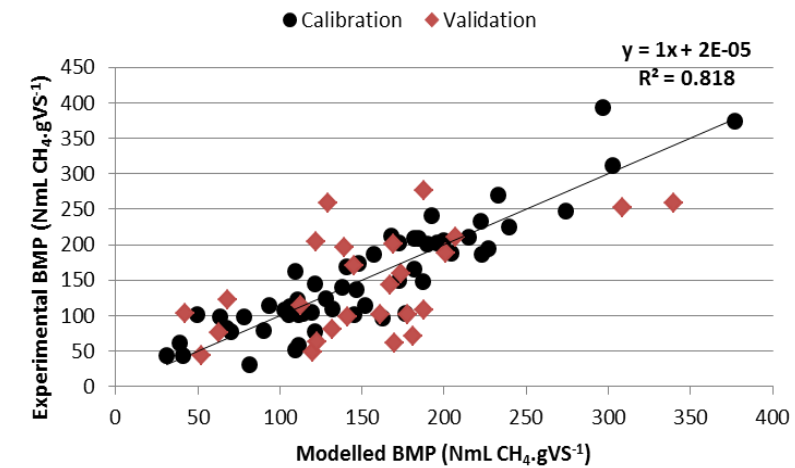
complexity



Anaerobic

Aerobic

Methane potential



Soil amendment potential